

01 Jan 1973

Measurements in Turbulent Water and Two-Phase Flows by Laser Anemometry

A. Melling

J. H. Whitelaw

Follow this and additional works at: <https://scholarsmine.mst.edu/sotil>

 Part of the [Chemical Engineering Commons](#)

Recommended Citation

Melling, A. and Whitelaw, J. H., "Measurements in Turbulent Water and Two-Phase Flows by Laser Anemometry" (1973). *Symposia on Turbulence in Liquids*. 107.
<https://scholarsmine.mst.edu/sotil/107>

This Article - Conference proceedings is brought to you for free and open access by Scholars' Mine. It has been accepted for inclusion in Symposia on Turbulence in Liquids by an authorized administrator of Scholars' Mine. This work is protected by U. S. Copyright Law. Unauthorized use including reproduction for redistribution requires the permission of the copyright holder. For more information, please contact scholarsmine@mst.edu.

MEASUREMENTS IN TURBULENT WATER AND TWO-PHASE FLOWS BY LASER ANEMOMETRY

A. Melling and J. H. Whitelaw
Imperial College of Science and Technology
Mechanical Engineering Department
Exhibition Road
London SW7 2BX, England

ABSTRACT

Measurements of the mean and rms values of the longitudinal velocity in a rectangular duct are reported. These results were obtained in a water flow using a laser anemometer. The important design criteria which facilitated the measurements are described and gradient, transit-time, noise and refractive-index corrections are specifically discussed. The results demonstrate the development of a rectangular duct flow and, in particular, reveal that a small lack of symmetry at the duct entrance can readily be identified in the normal-stress results, 37 hydraulic diameters downstream.

The possibility of utilizing water droplets in steam and gas bubbles in water to scatter light and thereby to assist laser-anemometer studies of turbulence is discussed. Experimental evidence obtained by the authors and their colleagues is used to support the conclusions.

INTRODUCTION

This paper has been prepared to communicate experience of applying laser-anemometry techniques to the measurement of mean and fluctuating velocity in water and two-phase flows and to present recent results obtained in water flows. It is hoped that the achievement of the former purpose will assist others to use laser-anemometry techniques and of the latter will stimulate its use for further investigations of turbulent flows.

It is well known that the principal advantages of laser anemometry are that it does not disturb

the flow where measurements are to be obtained and that the instrument has a linear response to one velocity component. These are particularly relevant to water flows where the usual instrument for measuring turbulence properties, the hot-film anemometer, does disturb the flow, requires that the water be clean, and has a non-linear response characteristic. The properties of water and the particles which it carries make it particularly suited to laser-anemometry measurements. In addition, because the measuring-control volume can be arranged to be particularly small, turbulence can in many cases be studied in water flows of small dimensions; however, a reduction in scattering volume size is normally accompanied by an increase in ambiguity noise which may limit the maximum turbulence frequency measurable. Of course, since laser anemometry requires the transmission and collection of light, windows are required and this may be considered a disadvantage.

To take advantage of the potential merits of laser anemometry, the components of the anemometer must be carefully designed. Relevant design criteria are indicated in DESIGN CRITERIA below together with the corrections which may require to be applied. Corrections for gradient-broadening, transit time, electronic noise, and refraction, which may result from the design of a test section and the optical arrangement, are described.

Water flows offer the advantages to laser anemometry that they are transparent, carry a large number of particles to scatter light and usually have significant turbulent energy only up to approximately

300 Hz. There is little direct knowledge of the size distribution of the particles carried by water but experience with different particles and optical-fringe spacings suggests that the number-mean diameter is of the order of $1\ \mu\text{m}$, with very few particles more than ten times larger. Assuming very conservative figures, namely a $5\ \mu\text{m}$ particle diameter with a density ratio of 10, fluctuations of 300 Hz will still be followed faithfully, as indicated by the analysis of Reference 1. The number density of these particles is very high in comparison with gas flows and with control-volume dimensions defined by an angle between the light beams of around 20° , the resulting signal can be arranged to be continuous, thereby facilitating the use of a frequency-tracking demodulator. If counting techniques are employed, the statistically required number of counts to evaluate mean and rms quantities within small confidence limits can be obtained in minimum time, but methods for triggering counters and validating their operation have been developed only for signals from individual particles.

The measurements described in this paper relate mainly to the flow of water in a rectangular duct and were obtained with the instrumentation described. As will be seen, a frequency-tracking demodulator was employed to process a signal from the rectangular-duct flow. Since the diagnosis of the rectangular-duct flow required a great many measurements, the use of a tracker with its direct read-out was particularly convenient.

Because of the importance of two-phase flow and present comparatively poor understanding, the Results Section includes a discussion of recent attempts to measure in bubbly flow and in wet steam. As will be indicated, measurement in bubbly flow is very difficult due to the nature of light scattering from large particles. In wet steam, with dryness fractions in excess of 95%, precise measurements of mean velocity were, however, obtained.

At the 1971 Symposium on Turbulence in Liquids, Dunning and Berman (2) in their papers on laser anemometry stated that "No set of measurements in

practical turbulent flows has been obtained to evaluate the instrument." This was a timely comment at that time, but now two years later, the situation is rather better. In addition to the measurements of Reference 2, measurements of mean and rms quantities have been obtained in fully-developed turbulent-channel flow (3), (4) and in free-jets (5), (6) and demonstrate that, with careful design and operation, the laser anemometer reproduces the results established previously by hot-wire techniques. In addition, and armed with this assurance, there have been several applications of the technique to industrially important problems. The reader is directed to References 7 to 10 for up-to-date reports on these activities.

DESIGN CRITERIA

It is only in exceptional cases that the fluid-dynamicist has complete control over the design of his laser anemometer. More often, his freedom of choice is limited to the design of some components and the purchase of others. This section has been prepared, therefore, in three parts. The first part is concerned with the statement and availability of guide lines for design and choice. The second part is concerned with sources of error and the form of the required corrections; in many cases, careful design and choice of components can obviate the need for some of the corrections. Comments of a practical nature and concerned with the operation of laser anemometers in near-wall regions and in the presence of secondary or reverse flows are provided in the third part.

Guide Lines for Design and Choice of Components

The components of a laser anemometer are indicated in Figure 1. They consist of a laser, an optical arrangement to provide two beams of focused light, a light collecting system which can define the measuring control volume, a photomultiplier or diode to convert the optical signal to an electronic signal and an electronic signal processing system. These components are considered in turn.

Laser and geometrical requirements have been discussed in References 11 and 12 and are summarized

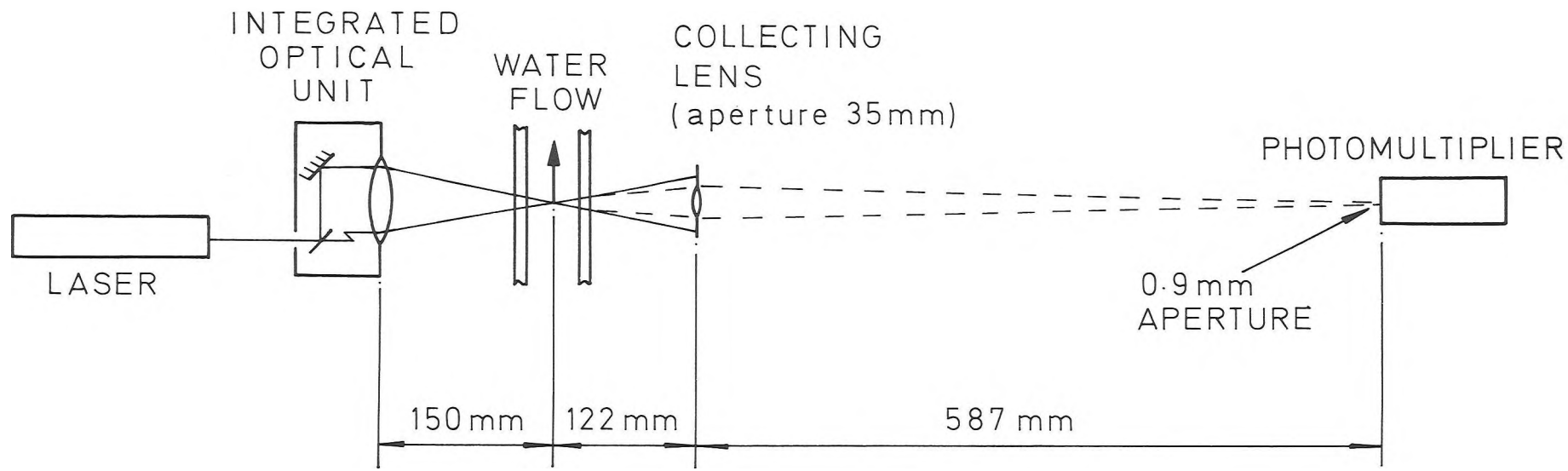


Figure 1. Components of laser anemometer.

here. The signal-to-noise ratio (SNR) of the Doppler signal is normally limited by the shot-noise process of electron emission from the photocathode, with a quantum efficiency η_q and a noise bandwidth Δf which can be taken as equal to the range of Doppler frequencies measured. The relationship

$$\text{SNR} \propto \frac{\eta_q \lambda}{\Delta f} \frac{d_p^2}{d_2^2} Q_{\text{scat}} P_\ell \quad (1)$$

indicates the advantage of increasing laser power P_ℓ , focusing the incident beams strongly to minimize d_2 , and using a small wavelength of laser light. The scattering coefficient Q_{scat} depends on d_p so a large particle diameter does not necessarily increase the SNR. Reflection losses at windows augment laser power requirements for given SNR.

The geometrical arrangement, should be designed in integrated form as proposed, for example, in References 3, 11, 13 and 14. Particle concentration dictates the use of reference-beam or fringe (dual scatter) anemometers (15), and the particle size determines the fringe spacing Δx (16, 17). In terms of the half-angle between the beams, ψ as measured in air or θ as measured in a liquid of refractive index m , and the wavelength, λ , in vacuo,

$$\Delta x = \frac{\lambda}{2 \sin \psi} = \frac{\lambda}{2m \sin \theta} \quad (2a)$$

The velocity is given by

$$U = v_D \Delta x \quad (2b)$$

The waist diameter of a focused Gaussian beam of initial diameter D_2 , measured between points of intensity $1/e^2$ of the maximum, is

$$d_2 = \frac{4}{\pi} \lambda \frac{f}{D_2} \quad (3)$$

thus the number of fringes in this region is

$$N_2 = \frac{d_2 / \cos \psi}{\Delta x} = \frac{8}{\pi} \frac{f}{D_2} \tan \psi \quad (4)$$

The number of fringes in the control volume may also be important to minimize transit-time broadening; this is discussed in the following sub-section.

The light-collecting system consists of a light-collecting lens and an aperture in front of the photomultiplier. The aperture dimension, d_{ph} , and the locations of the lens and aperture can control the magnification, M , of the image of the control volume and thus the size of the measuring control volume and the number of fringes observed by the photo-cathode. The control volume dimensions are linked to the geometry of the light collecting system by the equations

$$d_m = \frac{d_{\text{ph}}}{M} \quad (5)$$

and

$$\ell_m = \frac{d_w}{\sin \theta} \quad (6)$$

where d_m is the focused-beam diameter between points of minimum significant light intensity ($\approx 2\%$ of maximum). The number of fringes observed is

$$N_{\text{ph}} = \frac{d_m}{\Delta x} \quad (7)$$

The photomultiplier should be selected to maximize the quantum efficiency. Manufacturers' catalogs provide the necessary information. The authors have found that EMI Model 9558B (RCA equivalent model 7265) with S-20 spectral response is suitable for operation with He-Ne lasers and EMI Model 9656B (RCA equivalent model 8575) with S-11 spectral response for Argon lasers; alternatively EMI Model 9658R (S-20 response) is satisfactory in both cases. The photomultiplier high-voltage supply should be chosen to provide the appropriate current and voltage (e.g. 1 mA up to 1 kV) and with a ripple of less than 0.5 mV rms.

Signal analysis in liquid flows can conveniently be accomplished with similar precision using a frequency-tracking demodulator or a counter. The authors have used frequency trackers for almost all their measurements in water flows and the following brief comments are related, therefore, to instruments of this type. Three trackers have been used, i.e. those manufactured by DISA, Cambridge Consultants & Imperial College.

The DISA instrument contains a frequency-locked loop and is described in detail in Reference 18. The Cambridge Consultants instrument is similar to that of DISA but is more recently designed and is able to follow more rapid frequency changes. The Imperial College instrument was built around a Signetics phase-locked loop and operates on a null-detection principle. A comparison between the DISA and Cambridge Consultants instruments resulted in measurements of non-dimensional mean-velocity in the water flow described in Section 3 which had a maximum deviation of 1% and an average deviation of 0.4%; the corresponding maximum and average deviations for the rms measurements were 6% and 3.7% within regions of the flow with turbulence intensity less than 0.10. Comparison between the DISA and Imperial College instruments indicated for mean measurements a maximum deviation of 3% and an average deviation of 1.4% and, for rms measurements, maximum and average deviations of 8% and 4.5% for turbulence intensities below 0.08.

Correction Factors

The laser anemometer should, of course, be designed to minimize possible errors but, in general, the processed signal from the photomultiplier is not equivalent to velocity without correction. For the frequency-tracking demodulators referred to in the previous paragraph, and the range of the present measurements, errors due to non-linearity, slew rate and locking to or unlocking from a Doppler signal were negligible because of the low velocity and turbulence intensity. Errors due to the finite dimensions of the control volume leading to velocity-gradient and transit-time broadening were not always negligible and are considered below together with corrections made necessary by electronic noise and by refractive-index changes: the last named correction differs from the others in that it affects the location of measurement.

Gradient broadening - Reference 19 outlines a procedure for correcting mean velocities measured by laser anemometry in a flow with a spatially non-uniform velocity field and recommends corrections to measured rms levels. The error in measuring \bar{U} rather than U_0 at a point $x_2 = x_{2,0}$, when the dimension σ_{x_2} of the ellipsoidal scattering volume is

parallel to the predominant velocity gradient is approximately

$$\bar{U} - U_0 \approx \frac{\sigma_{x_2}^2}{2} \frac{\partial^2 U_0}{\partial x_2^2} + \frac{\sigma_{x_2}^4}{8} \frac{\partial^4 U_0}{\partial x_2^4} + \dots \quad (8)$$

and the velocity profile may be represented by the polynomial

$$U_0 = U_s \sum_{n=0}^N C_n \left(\frac{x_2 - 0}{D} \right)^n \quad (9)$$

The coefficients C_n and the necessary geometric parameters may be supplied to Equation 9 to yield the necessary correction. For the measurements reported below this correction was always negligible.

In Reference 19, Melling recommends that the procedure of Reference 20 be used in correcting the measured rms level. The appropriate equation is

$$\overline{(U - \bar{U})^2} = \left(\frac{\partial U}{\partial x_2} \right)^2 \sigma_{x_2}^2 \quad (10)$$

or for a frequency tracker and anemometer with voltage/velocity transfer function $E = KU$.

$$\left(\frac{\tilde{e}}{E} \right)_g = \frac{\partial U}{\partial x_2} \frac{\sigma_{x_2}}{U} \quad (11)$$

Transit-time Broadening - Due to the finite life-time of the signal associated with each scattering particle passing through the measuring control volume, the Doppler spectrum has a finite rms spectral width, σ_F , even in steady laminar flow. Finite transit time broadening has been discussed in a number of papers, e.g. References 21 to 24, the most comprehensive treatment being that of George and Lumley (24). The random arrival and departure of particles to and from the scattering volume causes fluctuations in phase, and hence frequency, of the Doppler signal. The phase fluctuations are correlated only over the transit time of particles across the volume, which depends on the velocity and a scattering volume dimension. The appropriate dimension suggested in Reference 24 is the standard deviation, $\sigma_{x_1} = d_2/4$, where the rms contribution to the Doppler

spectrum width from finite transit time is given (in rad/s) as

$$\sigma_F = \frac{U_1}{\sqrt{2}\sigma_{x_1}} \quad (12a)$$

In terms of a number of fringes the relative broadening can be expressed as

$$\frac{\sigma_F}{\omega_D} = \frac{\sqrt{2}}{\pi N_2} \quad (12b)$$

by combining Equations 12a, 2a and 2b. The appropriate dimension to be used in Equation 12a when the scattering volume is defined by an aperture [Equation 6], rather than the Gaussian light intensity distribution, is not certain, but it should be adequate to use σ_{x_1} if $d_m > d_2$.

Equation 12a suggests that finite transit time broadening could be minimized by enlarging the scattering volume, but this conflicts with requirements of good spatial resolution. The problem of optimizing the scattering volume dimensions to secure the best frequency response to turbulent velocity fluctuations is discussed in Reference 24 in terms of the energy spectrum of velocity fluctuations and an "ambiguity" spectrum, which arises from all broadening sources, including gradient and finite transit time broadening. Reducing the ambiguity spectrum to maximize the frequency at which it exceeds the turbulence spectrum will be limited by attenuation of the turbulence spectrum at high frequencies through spatial averaging as the scattering volume is enlarged. A single scattering volume cannot be optimized for all positions in a turbulent flow.

Adrian (21) and Greated and Durrani (22) have shown that the error due to transit-time broadening appropriate to FM-tracking demodulators is modified by the response time, T_a , of the feedback loop according to the equation

$$\left(\frac{\tilde{\epsilon}}{E}\right)_F \approx \frac{\sigma_F}{\omega_D} \left(4 \frac{\sigma_t}{T_a}\right)^{1/2} \quad (13)$$

where $\sigma_t = U_1/\sigma_{x_1}$, is an effective transit time and T_a is the time constant of the feedback loop of the tracker. If the loop time constant is presumed independent of ω_D , Equation 13 with Equation 12b and the definition of σ_t implies

$$\left(\frac{\tilde{\epsilon}}{E}\right)_F \propto E^{-1/2} \quad (14)$$

Figure 2 presents experiments which demonstrate qualitative agreement with Equation 14. They were obtained using an optical arrangement similar to that shown in Figure 1 and the DISA frequency-tracking demodulator on the axis of a fully-developed laminar flow of water in an 11mm diameter glass tube.

The Doppler frequencies extended over three ranges of the tracker, so the results are plotted on a common abscissa of tracker output voltage, where 10 volts corresponds to the maximum Doppler frequency of each range. The figure suggests that using the upper portion of a range should allow the error stemming from finite transit-time broadening to be reduced to about 0.5%. In turbulent flows, however, tracking is not easily achieved at the upper end of a range because of limitations imposed by the tracker's slew rate, i.e. the maximum rate at which frequency changes can be followed, and the dynamic range, i.e. the ratio of maximum to minimum trackable frequencies on each range of the tracker (Reference 36). In addition George and Lumley (24) state that the reduction in finite transit time fluctuations implied by Equation 13 when $T_a > 4\sigma_t$ cannot be achieved without filtering out some of the turbulent velocity fluctuations.

Electronic Noise - The three frequency-tracking demodulators discussed earlier in this section, had rms noise levels which were nearly constant. Relative to the mean voltage, however, these noise levels increased significantly towards the lower part of each frequency range. It is, therefore, preferable that tracking should be effected away from the lower part of a particular frequency range, although the rms level can be corrected for this noise if necessary. For the DISA tracker the electronic noise level, $\left(\frac{\tilde{\epsilon}}{E}\right)_n$, was at most 0.2%,

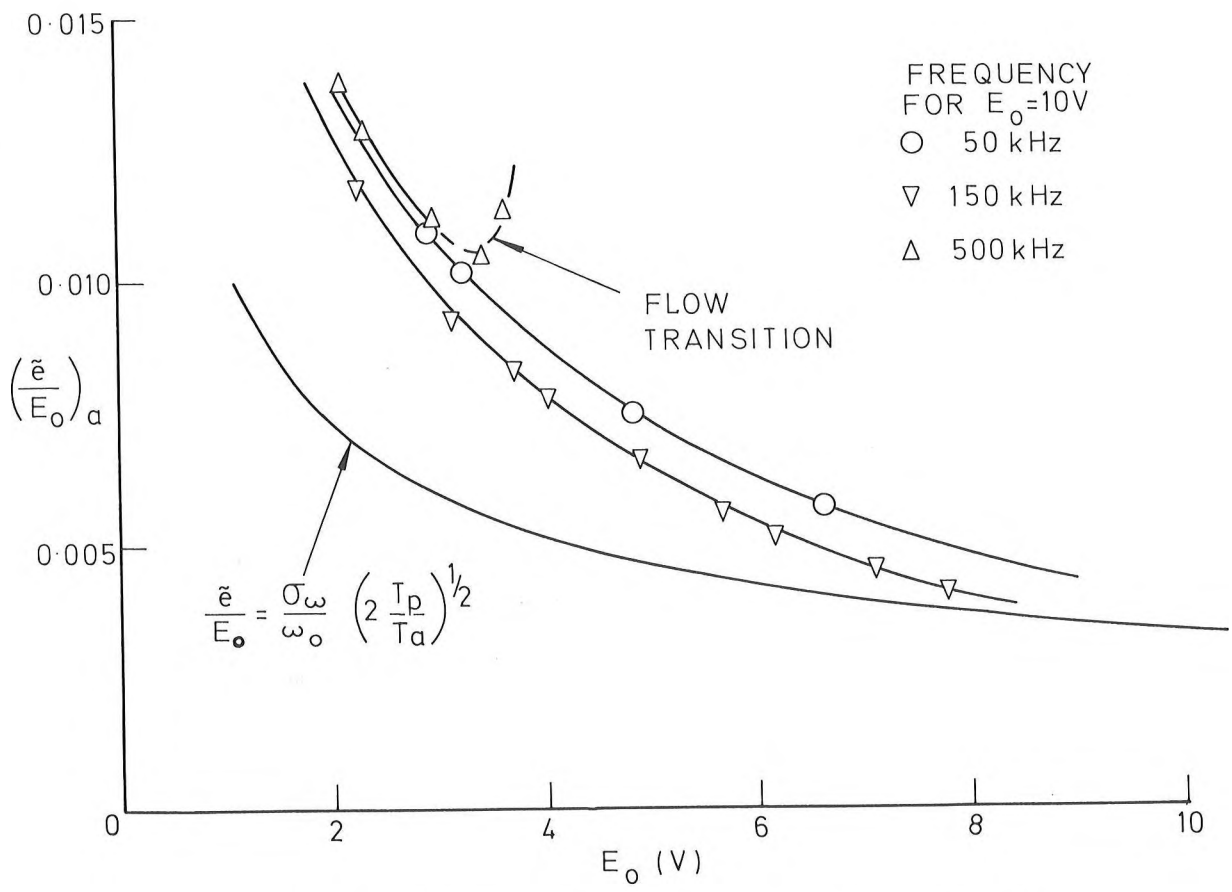


Figure 2. Measured and calculated values of transit-time.

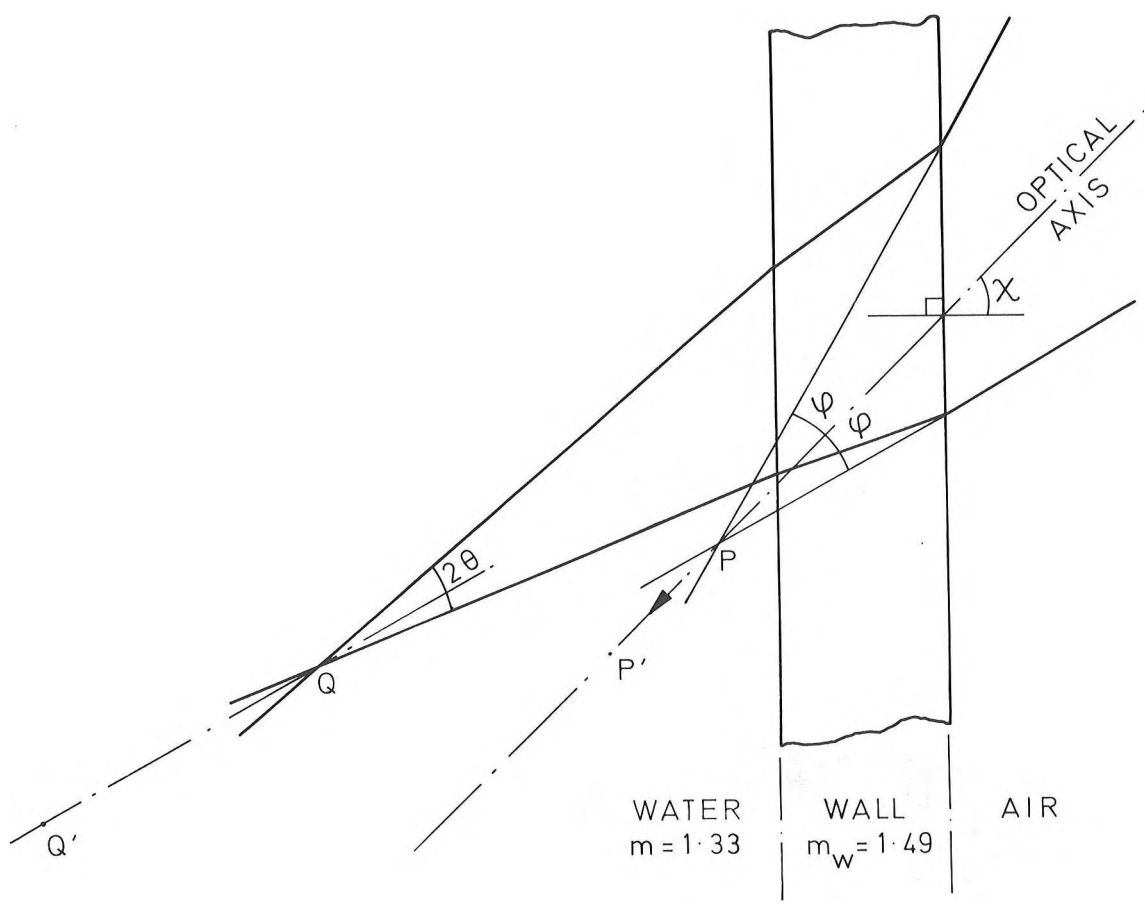


Figure 3. Refraction at walls.

The measured rms level, $\frac{\bar{e}}{E}$, thus combines the effects of turbulent velocity fluctuations, $(\frac{\bar{e}}{E})_t$, and the three other sources of voltage fluctuations just discussed. Assuming the probability-density function of the output voltage is symmetrical and Gaussian, the mean-square turbulence level is found from

$$\left(\frac{\bar{e}}{E}\right)_t^2 = \frac{\bar{e}^2}{E^2} - \left(\frac{\bar{e}^2}{E^2}\right)_g - \left(\frac{\bar{e}^2}{E^2}\right)_F - \left(\frac{\bar{e}^2}{E^2}\right)_n \quad (15)$$

Although the corrections are smaller in the regions of higher mean velocity, their influence can be greater in these regions because of the lower turbulence levels away from the duct walls.

Influence of refractive index - For most laser anemometry purposes, water flows are contained within glass or Plexiglas ducts. Since the refractive indices of water and Plexiglas are different from that of air, the focal point of the focussing lens does not correctly define the location of crossing of the two beams within the flow, and the beams no longer cross exactly at their waists. For the general case indicated in Figure 3, the coordinates of the crossing point Q in water relative to the focal point P of the lens are given by complicated trigonometric functions involving the wall thickness t, the distance from P to the wall, the refractive indices, m_w and m , of the wall and the water respectively, the angle, χ , between the optical axis and the normal to the wall, and the half-angle ψ between the beams in air. Q does not lie on the optical axis and as the optical system is moved relative to the duct along PP', Q moves obliquely to the original optical axis along QQ'. The total-angle between the beams in the water is given by

$$2\theta = \sin^{-1} \left(\frac{\sin(\chi + \psi)}{m} \right) - \sin^{-1} \left(\frac{\sin(\chi - \psi)}{m} \right) \quad (16)$$

For normal incidence, as used for all the measurements reported here, Q lies on the axis and moves a distance $x_{2,Q}$ when the optical system is traversed a distance $x_{2,P}$ such that

$$\frac{x_{2,P}}{x_{2,Q}} = \sqrt{\frac{1 - \sin^2 \psi}{m^2 - \sin^2 \psi}} \quad (17)$$

Equation 16 is replaced by

$$\sin \theta = \frac{\sin \psi}{m} \quad (18)$$

It should be noted that the thickness and refractive index of the wall do not affect the movement of the scattering volume if the axis of the optical system is normal to the wall.

Comments Relating to Near-wall Regions, Secondary and Reversed Flow

Two important aspects of velocity measurement in internal flows are those of measuring near walls and in regions of low mean velocity with high turbulence level, such as in separated or recirculating flow or in the secondary flows induced by turbulent normal stresses. For the first of these cases, two distinct difficulties may arise, namely swamping of the scattered light from particles with light scattered from the interface between the fluid and the wall, and presence of high turbulence and steep mean velocity gradients. Provided the scattering volume is more than 2 mm away from the wall lying between it and the photodetector, light scattered from the interface will not, with the present arrangement, be focused onto the photomultiplier aperture; aligning the optical system with the beams in a plane parallel to the wall near which the flow is to be studied will ensure that the small dimension of the ellipsoidal scattering volume lies across the velocity gradient thereby minimizing the gradient broadening and allowing near-wall measurements of velocity components parallel to the wall. Data on near-wall turbulence obtained by laser anemometry have been reported in References 33 and 34, in which the optical systems were arranged to minimize the scattering volume. In a three-dimensional flow the flow behavior near more than one wall is of interest and the scattering volume is bound to be disadvantageously aligned with respect to some confining surface, for example, in corners.

To detect velocity components normal to walls, it would be necessary to incline the optical axis to the wall, e.g. by running one incident beam parallel to the surface, in order to bring the scattering volume near the wall without blocking one of the beams.

Off-axis collection of the scattered light would also be necessary with precautions to shield the photodetector against reflection from the wall of the second incident beam. This arrangement can complicate the location of the measuring control volume, because of refraction and non-normal incidence.

Velocities within separated regions of flow and the transverse velocity components in a duct flow are commonly characterized by a low mean and large level of fluctuation, or, in other words, the velocity probability density function is centered near zero and extends to both positive and negative values. As a result, the Doppler spectrum is folded over on itself as both forward and reverse velocities give rise to "positive" frequencies; moreover, the Doppler spectrum interferes with the "zero frequency" spectrum from the low frequency pedestals of the Doppler signals associated with the presence of particles. A way to tackle the difficulty is to establish a steady state frequency difference between the two incident beams such that zero velocity is represented by a finite frequency with forward and reverse velocity fluctuations causing a rise above or fall below this basic frequency. Techniques to effect the necessary frequency shift of laser light are described and discussed in References 25 to 28.

EQUIPMENT AND RESULTS

The present measurements were obtained in the water flow in a rectangular duct of dimensions 40 mm x 41 mm and 1.8 m long. The flow configuration and instrumentation are described in the following subsection and the results presented thereafter together with comments relating to their precision and physical implications. The final subsection provides comments relevant to two-phase flows and particularly to recent investigations carried out by the authors and their colleagues; these two-phase flows provide indications of the applicability of laser anemometry to wet steam and bubbly flows.

Flow Configuration and Instrumentation

The present rectangular duct was located in a closed circuit as indicated on Figure 4. The water was pumped to a header tank and flowed into a 12:1 area-ratio contraction under the constant head provided by the overflow as indicated. This arrangement allowed a mass flow rate of up to 1.5 kg/s corresponding to a Reynolds number of 3.9×10^4 . Flow from the duct entered a second tank which was maintained full and overflowed into a sump.

The duct was constructed from 9 mm thick Plexiglas with a 125 mm long glass section inserted near the downstream end. This glass section was provided to allow the optical signal to be compared with that from the Plexiglas -confined region; in practice, the signal from the glass-confined region proved to be only marginally better. Scratches on the Plexiglas wall of the duct could cause serious deterioration of the signal; dirt was less serious but caused slow deterioration over a matter of weeks as it accumulated. The dimensions of the duct were measured at the position of the glass section and found to be within 0.2 mm of the nominal values given above.

The laser anemometer comprised a 5 mW helium-neon laser (Spectra-Physics Model 120), an integrated optical unit identical to that described in Reference 11, a 100 mm focal-length light-collecting lens, and a photomultiplier (EMI Model 9558B) preceded by an aperture. Figure 1 provides a line diagram of the optical arrangement and indicates the more important dimensions; Figure 5 represents a block diagram of the signal processing arrangements.

The anemometer was carried on a small milling table which allowed it to be traversed in the horizontal plane along the axis of the duct and orthogonal to this axis. Vertical adjustment was provided by jacking screws which raised or lowered the anemometer on the milling table. These adjustments, in conjunction with the two-channel optical unit indicated above allowed measurement of the axial and vertical components of velocity at any location in the duct. The duct and anemometer are shown on the photograph in Figure 6.

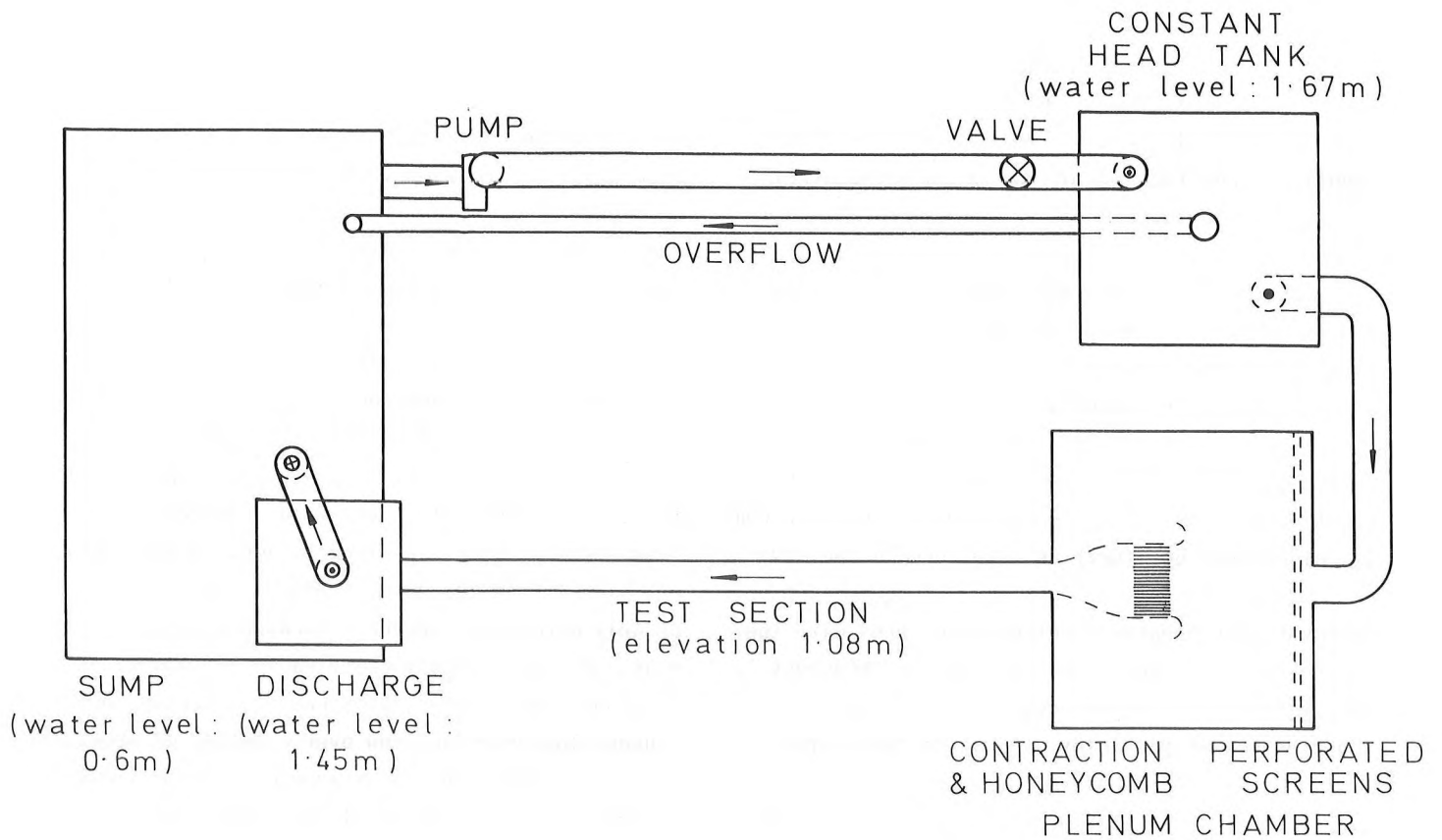


Figure 4. Line diagram of rectangular-duct, water-flow rig in plan view.

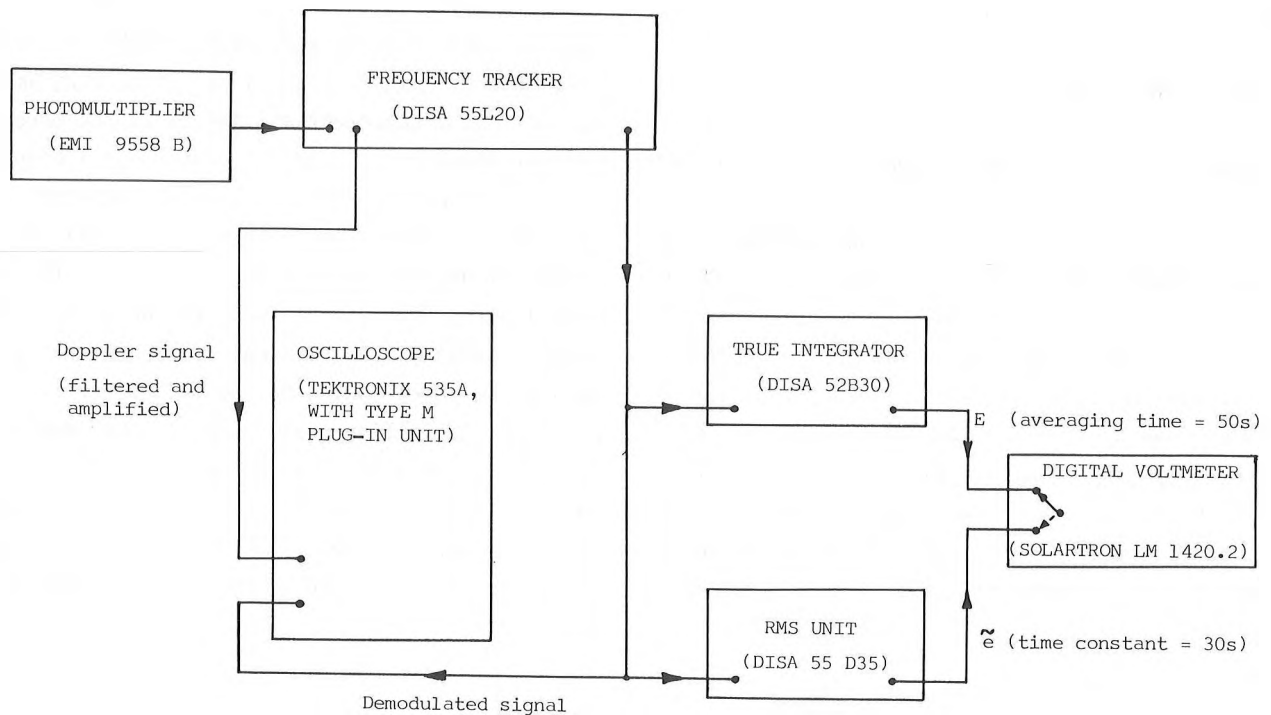


Figure 5. Signal processing electronics.

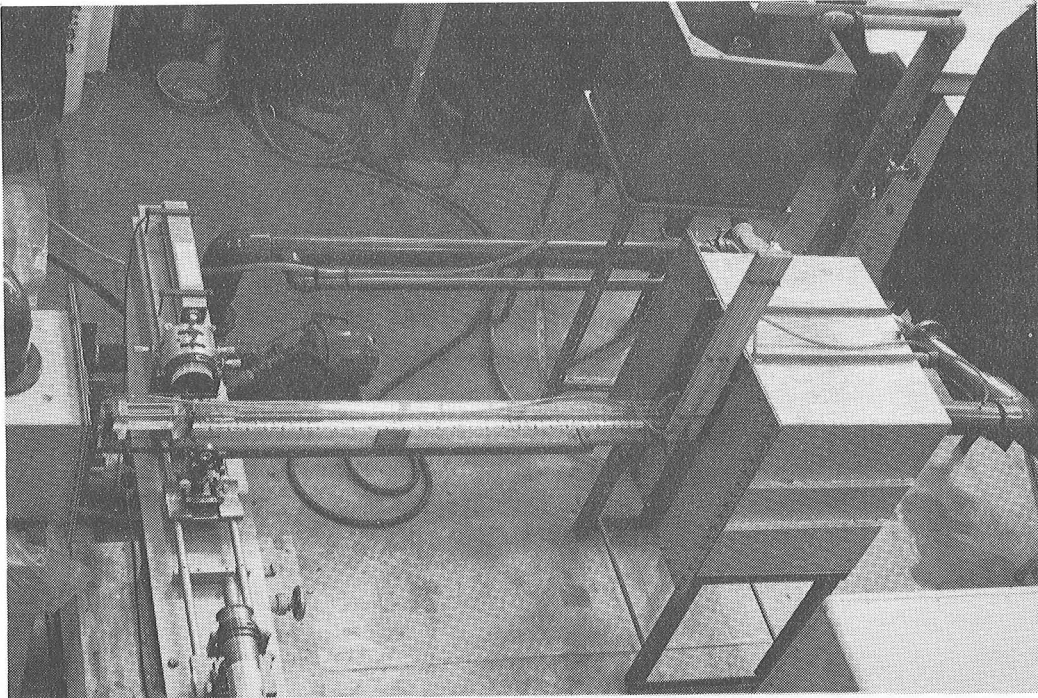
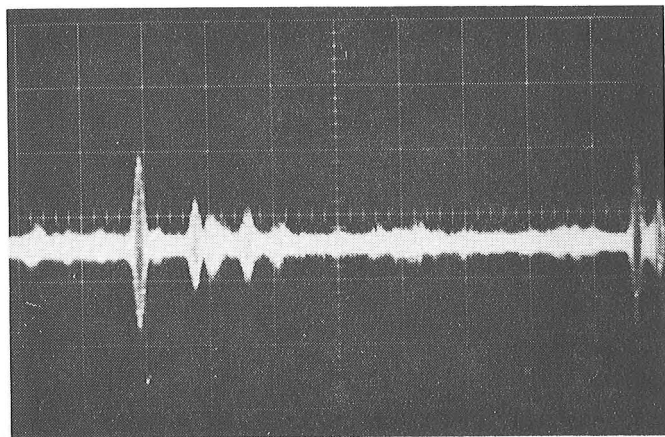
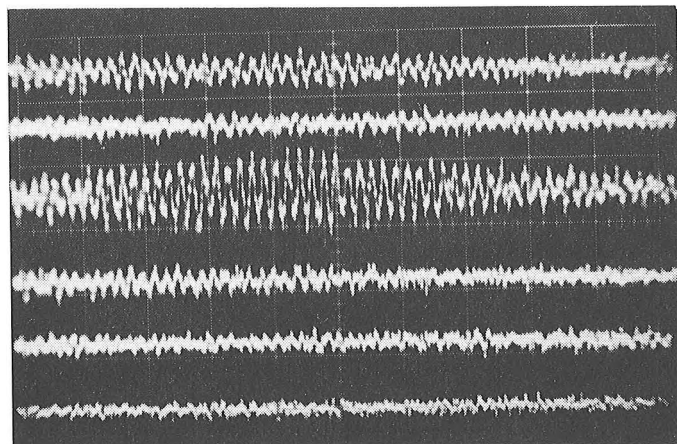


Figure 6. Photograph of water-flow rig and instrumentation.



(a)



(b)

Figure 7. Photograph of Doppler signal
a) 0.5 ms/div sweep rate
b) 10 μs/div sweep rate.

The present measurements were obtained with a focusing lens of 150 mm focal length. This, together with the properties of the laser beam and the 50.8 mm beam separation created by the optical unit, implied that the crossing region of the beams (at the 1/e intensity level) was 0.13 mm in diameter and 1.03 mm long and that the fringe spacing was 1.86 μm . The light-collecting dimensions indicated on Figure 1 ensured that 100 fringes were observed corresponding to a measuring control volume of 0.19 mm diameter and 1.45 mm length.

Results Obtained from Measurements in Duct

Typical signals obtained from the photomultiplier, appropriate to the water flowing in the rectangular channel, are shown on Figure 7. These signals were obtained from a location close to the center of the duct and 1.18 m from the entrance plane. They have been band-pass filtered between about 100 kHz and 2 MHz. The oscilloscope traces are typical of many which were photographed.

The signal traces suggest that the measuring control volume contained particles, capable of scattering measurable quantities of light, at all times. The DISA tracker, used for the present measurements, was operated with the minimum discrimination level which resulted in a signal drop out of under 2%. The probability that two particles, giving Doppler signals of large amplitude (Figure 7a) were present in the control volume at one time was small, although it is likely that the small amplitude signals of Figure 7b were in some cases the result of multi-particle scattering. The phase shift associated with the overlap of the two signals has been viewed by George and Lumley (24), for example, as the origin of transit time broadening due to the random arrival of particles in the scattering volume. An estimate of the magnitude of the errors discussed above and appropriate to the present results is provided below.

The quality of the signal shown on the trace may be partly judged by the relative levels of signal and noise. A better estimate was provided by the unfiltered signal which indicated a visibility of about 0.2, i.e. the ratio of Doppler modulation amplitude to the amplitude of the low frequency pedestal signal associated with particle presence.

The instrumentation shown on Figures 1 and 5 together with signals of the type shown on Figure 7 led to the measurements of mean frequency shown on Figure 8. The results were obtained in the indicated horizontal planes at a location corresponding to x_1/D_H of 37 and to a Reynolds number of 3.9×10^4 based on the bulk velocity and the hydraulic diameter. These results have been corrected for position using Equation 17; errors due to mean velocity gradient are negligible. The figure shows that, in terms of mean frequency and mean velocity, the flow has an asymmetry about the x_3 -plane of up to 7.5 kHz (15 mm/s) for $x_3/D < 0.6$ and 14 kHz (28 mm/s) overall.

From Figure 8, mean velocities can be deduced from Equation 2 in the form

$$U = \frac{v_D \lambda}{2 \sin \psi} \quad (19)$$

and corresponding contour plots are shown on Figure 9. Similar measurements, obtained at x_1/D_H of 5.6, are shown in contour-plot form on Figure 10. The contours of constant velocity (isovels) at x_1/D_H of 5.6 show that the symmetry of the flow is satisfactory apart from a small distortion which is evident along the positive and negative arms of the x_2 -axis. This distortion is less evident at x_1/D_H of 37 where the contour plots appear to be similar in each half quadrant. The bulges in the contours at the diagonals at the downstream location are expected and result from the secondary flows driven by the Reynolds normal stresses u_2^2 and u_3^2 . However, the pinching of the isovels along $x_3 = 0$ at the upstream position has caused the isovels to be more nearly parallel to the top and bottom walls than to the side walls.

Corresponding to the mean-frequency values shown on Figure 8, rms-frequency values normalized by the mean Doppler frequency at the duct axis are presented on Figure 11: these have not been corrected for gradient or transit-time or noise errors. A sample of six measurements was examined and indicated that the rms velocity, \tilde{u}_1/U , could differ from \tilde{v}_D/v_D by between 0.0006 and 0.0020 for \tilde{u}_1/U between 0.04 and 0.09. The results indicate that the turbulence intensity exceeds 10% only close to the wall. Once again, contour plots can be obtained and these are presented on Figures 12 and 13; they correspond to

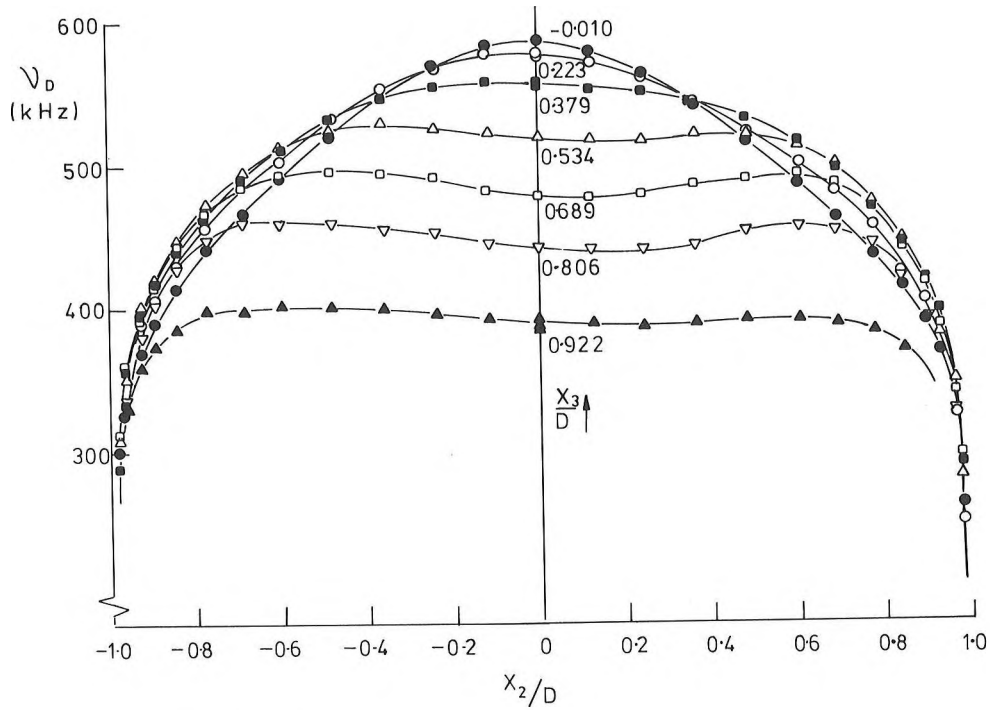


Figure 8. Mean-frequency profiles at $x_1/D_H = 37$

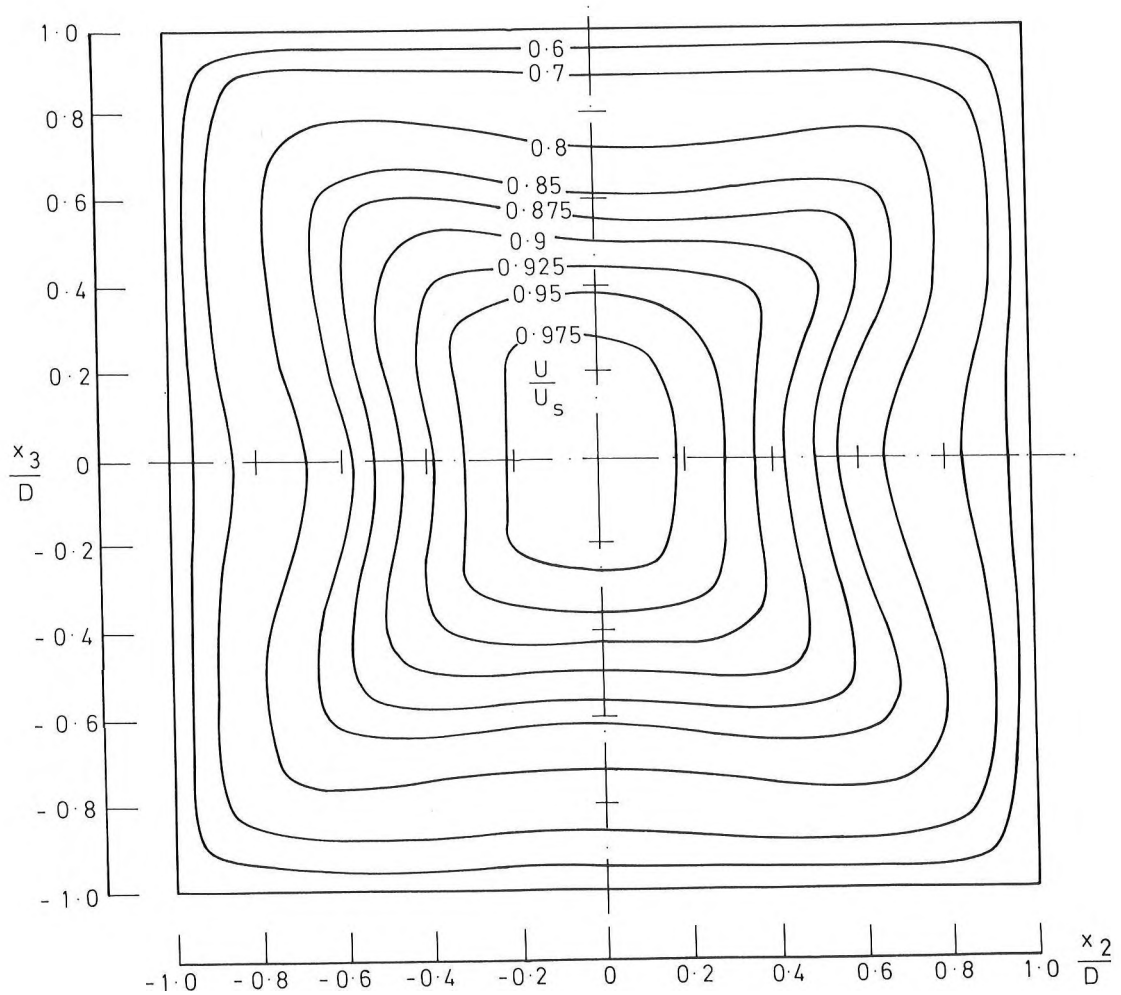


Figure 9. Contour plot of mean-velocity values at $x_1/D_H = 37$

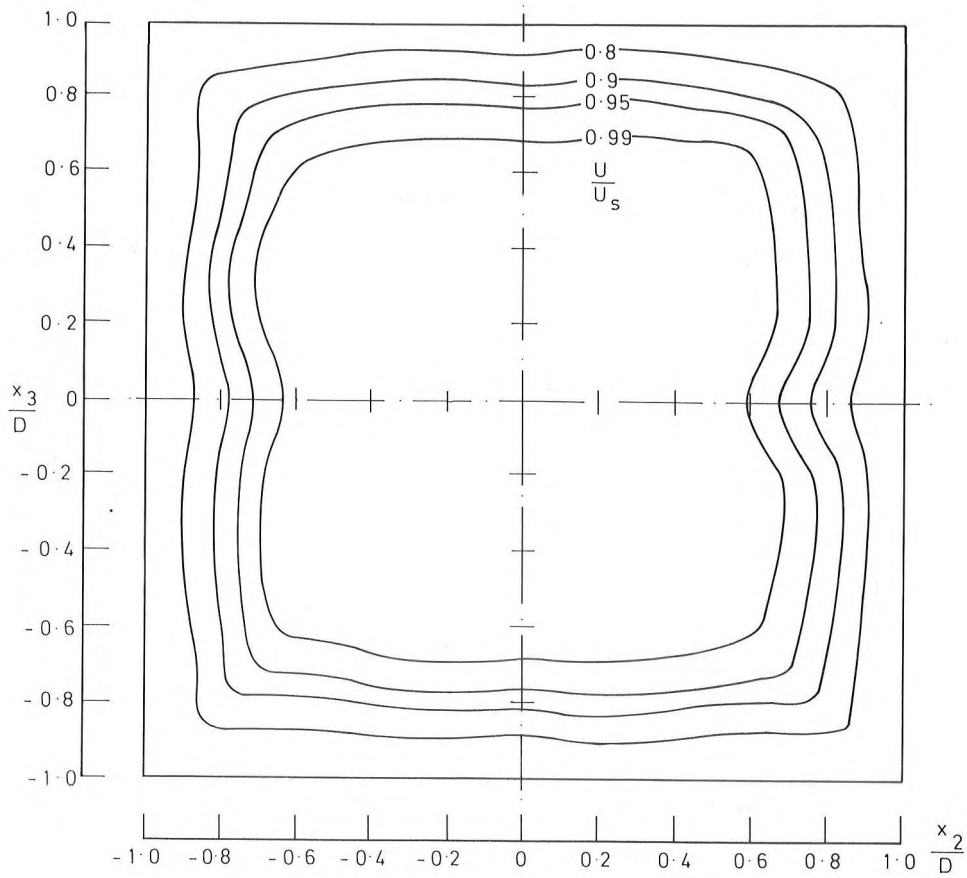


Figure 10. Contour plot of mean-velocity values at $x_1/D_H = 5.6$

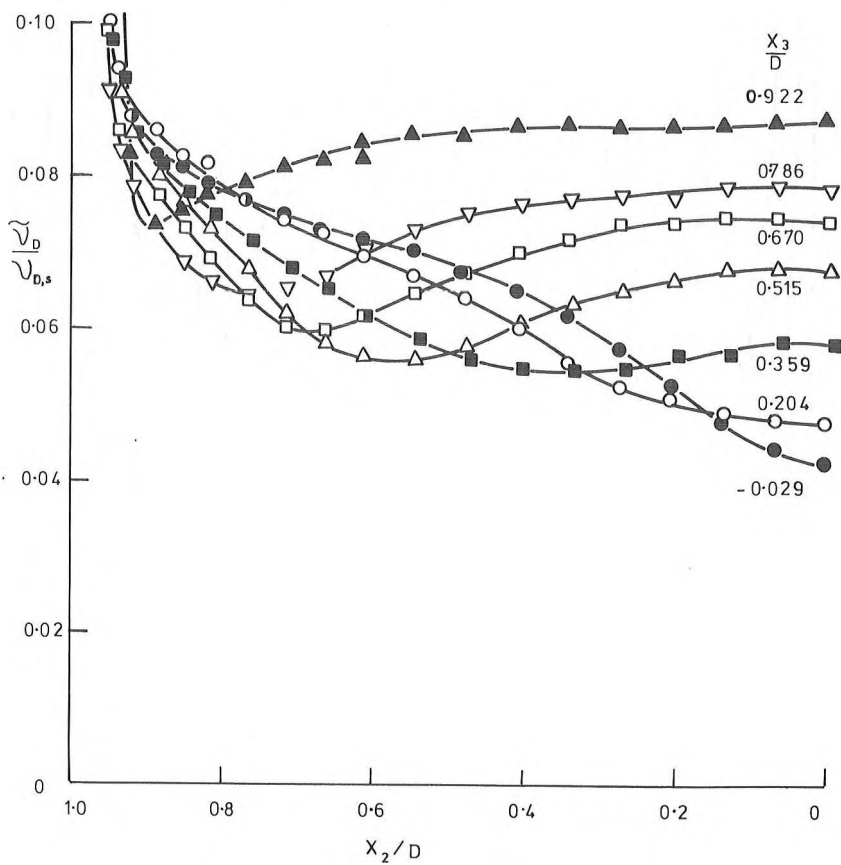


Figure 11. rms-frequency Profiles at $x_1/D_H = 37$

the contour plots of mean velocity presented earlier. The contour plot of rms values obtained at x_1/D_H of 5.6 shows a similar asymmetry to that observed on Figure 10: the protrusion revealed by the mean-velocity results has a counterpart in the rms values. At x_1/D_H of 37, the rms values reveal a related asymmetry and it is clear that, as revealed by the mean-velocity results, the slight asymmetry present in the flow at x_1/D_H of 5.6 has been carried through to x_1/D_H of 37.

The results presented above reveal the difficulties involved in attempting to arrange a symmetrical, rectangular-duct flow and the need for detailed contour plots to diagnose the existence of asymmetry. In the present case, the asymmetry stemmed from a slight non-uniformity in the honeycomb upstream of the contraction, in line with the x_2 -axis. A more symmetrical set of results is being obtained using a new honeycomb flow straightener and these will be corrected in accordance with the preceding formulae.

Measurements in Gas/Liquid Two-phase Flows

Measurements were obtained in wet-steam flows (29) using a laser anemometer similar to that described above but with laser powers up to 250 mW obtained from a Spectra-Physics (Model 165) argon-ion laser with Model 589 etalon, and a 300 mm focal length lens in the optical unit. A Hewlett Packard spectrum analyzer (Model 8552A/8553B) was used for signal processing. A 152 mm wide by 305 mm high steam tunnel carried the exhaust from a Curtis-type impulse turbine and Schlieren-glass inserts, 28 mm thick, located in the side walls of the tunnel facilitated the measurements. The flows used for the investigation covered a range of test-section pressures from 0.05 to 0.28 bar, velocities from 50-200 m/s and steam qualities from dry saturated to a dryness fraction of 0.95. Previous tests had indicated that the water droplets had a Sauter (volume-to-surface) mean diameter between 0.5 and 2 μm with the most probable diameter considerably smaller.

By assuming the particles to be monodisperse, the calculated number concentration of 0.5 μm particles at 0.1 bar pressure and 0.99 dryness

fraction implied that several hundred droplets were simultaneously in the measuring volume, although only a few droplets would be present if they were monodisperse and 2 μm in diameter. Observation of the signals from the photomultiplier suggested that the droplet concentration was closer to that calculated for 2 μm droplets, but at lower dryness fractions the droplet concentration in the scattering volume was certainly of the order of hundreds. This feature combined with the high Doppler frequencies involved, resulted in a poor quality signal although the frequency was resolvable by spectrum analysis. At such droplet concentrations it is possible that a reference beam system would have given better signals than the fringe system used, in line with Drain's (15) considerations; preliminary tests did not confirm this, but a conclusive comparison of the two systems was not obtained. The incident beams and, more importantly, the scattered light, were probably attenuated by secondary scattering from droplets outside the measuring volume and by large drops of condensate moving across the windows. Since the scattering volume was 75 mm from the windows there was fortunately no problem of light scattered by these large drops being focused on to the photodetector.

The measurements were undertaken to assess the possibility of calibrating pitot tubes in wet steam flows; thus only mean velocities were of interest. The flow had a low turbulence level, not exceeding 1%. Simultaneous measurements with the laser anemometer and pitot tube over the velocity range 150 to 200 m/s for dryness fractions between 0.99 and 0.95 agreed within the experimental errors, $\pm 1.1\%$ and $\pm 1.0\%$, for the respective instruments. The success obtained indicates that turbulent wet steam flows could be investigated by laser anemometry at least for dryness fractions in excess of 0.98, where droplet concentrations are not too high. However, because of the low pressure the droplets do not move in a continuum and the frequency response calculation of Reference 1 must be modified to account for a significant Knudsen number as in Reference 29. For a 1 μm droplet in vapor at 0.1 bar pressure, its amplitude response relative to the vapor is predicted to be 0.996 at 1 kHz and down to 0.75 at 10 kHz. For

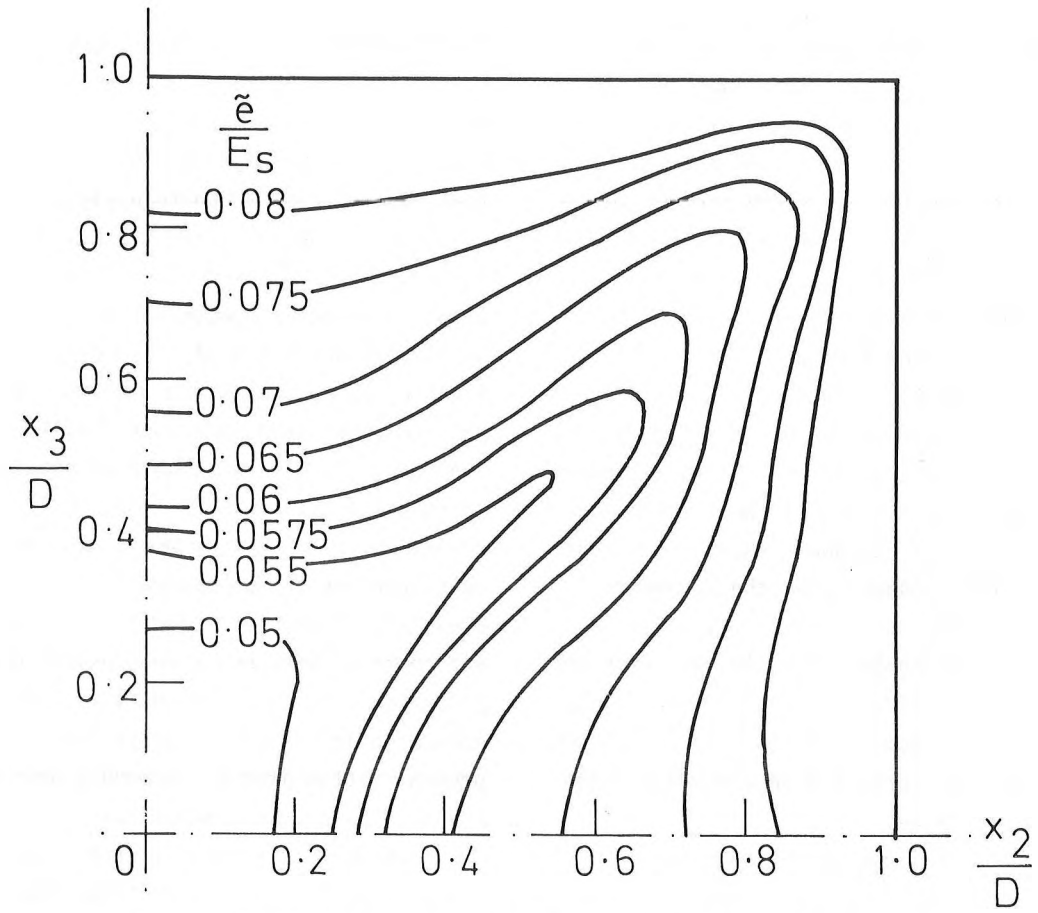


Figure 12. Contour plot of rms-velocity values at $x_1/D_H = 37$

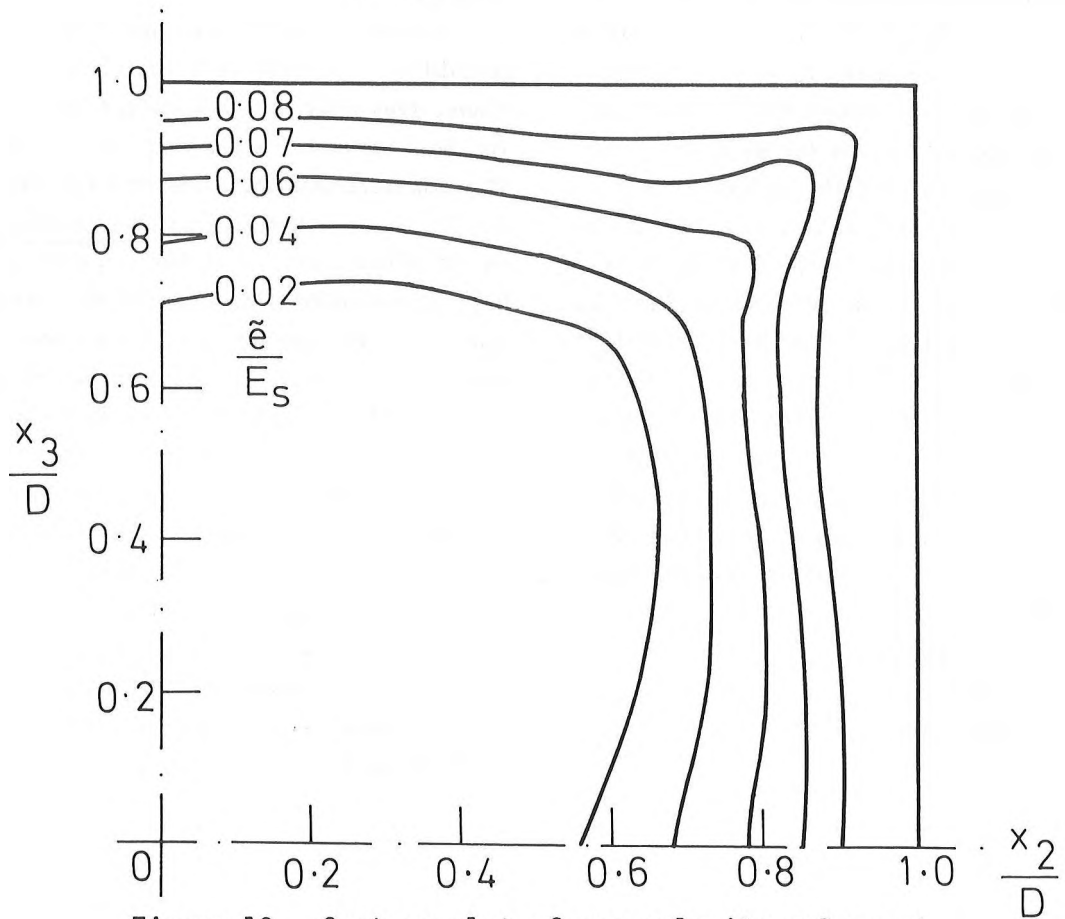


Figure 13. Contour plot of rms-velocity values at $x_1/D_H = 5.6$

a 2 μm diameter droplet the response is attenuated to 0.969 at 1 kHz. High frequency resolution of the vapor motion thus seems unlikely to be achieved, and mean velocities measured with larger droplets in accelerating flow may be in error because of particle velocity lag. The evidence suggests, therefore, that the water droplets found at the turbine exit can be used to scatter light and thereby to aid investigations of turbulence although the higher frequencies present in the flow may not be recognized.

Preliminary measurements in bubbly gas-water flow by Briard (31) indicated considerably greater problems than those experienced in the wet steam flow. Tests were made with bubbles rising by buoyancy through a downward flow of water. Both air bubbles and hydrogen bubbles were used, the latter being smaller and more evenly distributed throughout the flow, but in both cases the bubbles were too large to give Doppler signals in the forward-scatter fringe system used. Signals from contaminant particles in the water were obtained, except when a bubble blocked one or both of the incident beams, but the Doppler spectrum showed an extremely wide distribution of frequencies, indicative of high turbulence levels in the bubble wakes. Even had signals been received from the bubbles, the rate at which they crossed the anemometer scattering volume was very low and so statistically significant Doppler spectra would not be obtained in acceptable measuring times. In Reference 35, some measurements of the separate phases in bubbly flow were obtained by detecting back-scattered light from the bubbles and forward-scattered light from the water, an arrangement which showed considerable promise. As the diameters of the bubbles decrease and their number density in the liquid increases, measurements will become more precise. With very small bubbles, their motion should be indistinguishable from that of the liquid, a fact employed, of course, for hydrogen-bubble visualization studies of the type carried out in Reference 32. It is tempting to think that laser-anemometry procedures, using scattering from the hydrogen bubbles and from the water, could be used to quantify any lag of the bubbles relative to the liquid.

CONCLUSIONS

(1) The criteria required to design a laser anemometer for use in water flow are available, and if correctly implemented can lead to precise measurements of mean velocity and rms fluctuations, as well as avoiding calibration difficulties associated with hot-film anemometry.

(2) Water is a particularly convenient fluid for laser-anemometry technique because of its transparency, the adequate concentration of naturally-occurring particles able to scatter light and to follow the flow, the comparatively low frequency of the turbulence fluctuations, and the ability to use frequency trackers for signal processing.

(3) Extensive velocity measurements have been made in the developing turbulent flow in a rectangular duct. Initial asymmetry in the mean flow was still distinguishable 31 hydraulic diameters downstream. The corresponding rms values reveal more clearly that the asymmetry was recognizable at the downstream location. A large number of measurements was required to define the isovels and these were facilitated by the use of a frequency tracking demodulator. Except in regions of very low turbulence intensity, e.g. at the edges of the boundary layers in the developing flow, the uncorrected rms turbulence levels were very close to the levels found after accounting for the finite scattering volume dimensions.

(4) Exploratory measurements were made in two-phase flows of two kinds: water droplets in steam, and bubbles in water. In the former case the two phases moved together, while in the latter case the average relative velocity exceeded the velocity of either phase. Mean velocity measurements in wet steam were successful and, together with evidence of droplet size, suggest that turbulence measurements at high dryness fractions can also be successfully achieved; those of gas bubbles in water were a near-failure emphasizing the difficulties of measuring the velocities of scatterers of widely different size (bubbles, and particles in the water).

(5) The inherent advantages of laser anemometry should lead to its widespread use in turbulent liquid

flows, including those with swirl, polymer additives, flow separation, free surfaces, and, perhaps, two phases. The successful application of laser anemometry does, however, require that instruments be carefully designed and used with a knowledge of the relative advantage of the various possible optical and electronic systems and of the possible sources of error.

SYMBOLS

d_{ph}	diameter of aperture in front of photomultiplier
d_m	diameter of control volume
d_p	diameter of particle
d_2	diameter of waist of focused laser beam between $1/e^2$ intensity locations
d_w	diameter of waist of focused laser beam between locations of minimum significant intensity, e.g. 2% of maximum
D	half-width of duct
D_2	diameter of unfocused laser beam between $1/e^2$ intensity locations
D_H	hydraulic diameter of duct
\tilde{e}	rms voltage of the signal from the frequency tracker ($\sqrt{e^2}$)
E	voltage output from frequency tracker, instantaneous or mean
f	focal length
l_m	length of control volume
m	refractive index of water
m_w	refractive index of confining wall
M	magnification of light collecting arrangement
N	number of fringes within the measuring control volume
N_{ph}	number of fringes observed by the photocathode
N_2	number of fringes between $1/e^2$ intensity locations
P_ℓ	laser power
Q_{scat}	scattering cross-section

T_a	response time of feed back loop of frequency-tracking demodulator
t	wall thickness
U	longitudinal velocity component (in direction x_1) instantaneous or mean
\bar{U}	spatial mean value of U over scattering volume
U_0	value of U at center of scattering volume
U_s	normalization velocity
U_b	bulk velocity
\tilde{u}_1	rms longitudinal velocity component
x_1	} orthogonal coordinate system
x_2	
x_3	
Δf	noise bandwidth
Δx	fringe spacing
$x_{2,0}$	value of x_2 at center of scattering volume
χ	angle between optical axis and the normal to the wall
θ	half angle between light beams in water
ψ	half angle between light beams in air
λ	wave length of laser light
η_q	quantum efficiency of photo detector
σ_t	effective transit time
σ_x	rms dimension of scattering volume with Gaussian light intensity
σ_F	rms width of spectrum due to finite life time of signal
$\tilde{\nu}_D$	rms value of Doppler frequency
ν_D	Doppler frequency, instantaneous or mean
ω_D	Doppler frequency (rad/s), $\omega_D = 2\pi \nu_D$

SUBSCRIPTS

F	relating to transit time
g	relating to gradients in velocity
n	relating to noise
t	relating to turbulence
o	relating to center of scattering volume

REFERENCES

1. A. Melling and J. H. Whitelaw, "Seeding of Gas Flows for Laser Anemometry," *DISA Information*, 15, 5 (1973).
2. J. W. Dunning and N. S. Berman, "Turbulence Measurements Using Laser Doppler Velocimeter," *Proc. Symposium on Turbulence in Liquids*, Cont. Ed. Series, U. of Missouri, Rolla, 1971.
3. F. Durst and J. H. Whitelaw, "Integrated Optical Units for Laser Anemometry," *J. Phys.*, E4, 804 (1971).
4. W. J. Yanta and R. A. Smith, "Measurements of Turbulence-Transport Properties with a Laser-Doppler Velocimeter," *AIAA Paper* 73-169.
5. F. Durst and J. H. Whitelaw, "Measurements of Mean Velocity, Fluctuating Velocity and Shear Stress Using a Single Channel Anemometer," *DISA Information*, 12, 11 (1971).
6. D. Durao and J. H. Whitelaw, "Some Performance Characteristics of the Cambridge Consultants Frequency-Tracking Demodulator." Report available from Cambridge Consultants Ltd., Bar Hill, Cambridge, England, 1973.
7. W. H. Stevenson and H. D. Thompson, "The Use of the Laser-Doppler Velocimeter for Flow Measurements," *Project SQUID Report*, 1972.
8. F. Durst, A. Melling, and J. H. Whitelaw, "Laser Anemometry: A Report on EUROMECH 36, *J. Fluid Mech.*, 56, 143 (1972).
9. T. S. Durrant and C. Greated (Ed.), "Electro-optic Systems in Flow Measurement," *Proceedings of Symposium at the University of Southampton*, September 1972.
10. J. H. Whitelaw, "Laser Anemometry in Liquids and Gases," *Proc. Summer School on Measurement Techniques in Fluid Flows*, Ermenonville Castle, Paris, September 1973.
11. F. Durst and J. H. Whitelaw, "Light Source and Geometrical Requirements for the Optimization of Optical Anemometry Signals," *Opto-electronics*, 5, 137 (1973).
12. W. M. Farmer and D. B. Brayton, "Analysis of Atmospheric Laser Doppler Velocimeters," *Appl. Optics*, 10, 2319 (1971).
13. K. A. Blake and K. I. Jespersen, *The NEL Laser Velocimeter*, NEL Report No. 510, 1972.
14. D. B. Brayton, H. T. Kalb, and F. L. Crosswy, "Two-Component, Dual-scatter Laser Doppler Velocimeter with Frequency Burst Signal Read-out," *Appl. Optics*, 12, 1145 (1973).
15. L. E. Drain, "Coherent and Non-coherent Methods in Doppler Optical Beat Velocity Measurement," *J. Phys.*, D., 5, 481 (1972).
16. F. Durst, "Scattering Phenomena and Their Application in Optical Anemometry," *ZAMP*, 24, 619 (1973).
17. W. M. Farmer, "The Interferometric Observation of Dynamic Particle Size, Velocity, and Number Density," Ph.D. Thesis, Univ. of Tennessee, 1973.
18. M. O. Deighton and E. A. Sayle, "An Electronic Tracker for the Continuous Measurement of Doppler Frequency from a Laser Anemometer," *DISA Information*, 12, 5 (1971).
19. A. Melling, "The Influence of Velocity Gradient Broadening on Mean and rms Velocities Measured by Laser Anemometry," Imperial College, Dept. of Mech. Eng. Report HTS/73/33, (1973).
20. R. J. Goldstein and R. J. Adrian, "Measurement of Fluid Velocity Gradients Using Laser-Doppler Techniques," *Rev. Sci. Inst.*, 42, 1317 (1971).
21. R. J. Adrian, "Statistics of Laser Doppler Velocimeter Signals: Frequency Measurement," *J. Phys.*, E., 5, 91 (1972).
22. C. Greated and T.S. Durrani, "Signal Analysis for Laser Velocimeter Measurements," *J. Phys.* E., 4, 24 (1971).
23. C. P. Wang, "Effect of Doppler Ambiguity on the Measurement of Turbulence Spectra by Laser Doppler Velocimeter," *Appl. Phys. Lett.*, 22, 154 (1973).
24. W. K. George and J. L. Lumley, "The Laser-Doppler Velocimeter and its Application to the Measurement of Turbulence," *J. Fluid Mech.*, 60, 321 (1973).
25. W. H. Stevenson, "Optical Frequency Shifting by Means of a Rotating Diffraction Grating," *Appl. Optics*, 9, 649 (1970).
26. L. E. Drain and B. C. Moss, "The Frequency Shift of Laser Light by Electro-optic Techniques," *Opto-electronics*, 4, 429 (1972).
27. R. J. Baker, P. Hutchinson, and J. H. Whitelaw, "Detailed Measurements of Flow in the Recirculation Region of an Industrial Burner by Laser Anemometry," *Combustion Institute European Symposium*, Paper 97, 1973.
28. W. M. Farmer and J. O. Hornkohl, "Two-component, Self-aligning, Laser Vector Velocimeter," *Appl. Optics*, 12, 2636 (1973).
29. R. I. Crane and A. Melling, "Velocity Measurements in Wet Steam Flows by Laser Anemometry and Pitot Tube," *Central Electricity Research Laboratories Report RD/L/N 158/73*, 1973. To be published in *J. Fluids Eng.*
30. R. I. Crane and M. J. Moore, "Interpretation of Pitot Pressure in Compressible Two-phase Flow," *J. Mech. Eng. Sci.*, 14, 128 (1972).

31. P. Briard, "Laser Anemometry in Single and Two-phase Flows," M.Sc. Thesis, Imperial College, Univ. of London, 1971.
32. H. T. Kim, S. J. Kline, and W. C. Reynolds, "The Production of Turbulence Near a Smooth Wall in a Turbulent Boundary Layer," *J. Fluid Mech.*, 50, 133 (1971).
33. M. J. Rudd, "Velocity Measurements Made With a Laser Dopplermeter on the Turbulent Pipe Flow of a Dilute Polymer Solution," *J. Fluid Mech.*, 51, 673 (1972).
34. M. E. Karpuk, "A Laser Doppler Anemometer For Viscous Sublayer Measurements," M.S. Thesis, Oklahoma State Univ., 1974.
35. W. E. R. Davies and J. I. Unger, "Velocity Measurements in Bubbly Two-phase Flows Using Laser-Doppler Anemometry," Univ. of Toronto, UTIAS TN184, 1973.
36. D. F. G. Durão and J. H. Whitelaw, "Performance Characteristics of Two Frequency-tracking Demodulators and a Counting System: Measurements in an Air Jet," Proc. Second International Workshop on Laser Velocimetry, Purdue University, 1974.

ACKNOWLEDGMENT

The authors gratefully acknowledge the Central Electricity Generating Board for the financial support which made this paper possible.

DISCUSSION

H. M. Nagib, Illinois Institute of Technology: What do you think about applications of laser anemometry in combustion problems with high temperatures and so forth?

Whitelaw: There is a great deal that can be done in combustion situations. There are also limitations. I will mention the limitations and leave it at that. For example, measurements were obtained in a furnace which was 2 meters in diameter. If you take a laser beam and shine it across the refractive index gradients what you get in a furnace of that size is a very substantial attenuation of the beam. It increases in diameter and you don't get the intensity. We got measurements, however, in that furnace and then we measured in a furnace which was 16 feet across and we encountered

very severe difficulties because (I think) the beam is attenuated and fluctuates in space so much that we have gone past the point of no return. My conclusion from that is that the refractive index gradients which exist in combustion systems due to the density changes and the temperature changes in the flow can cause problems. These problems are associated with the distance over which you have to traverse the beam and I think there will be a limit to what we can do.

R. J. Hansen, Naval Research Lab: Can situations such as you have described, in which difficulty is experienced in making laser anemometer measurements due to refractive index gradients and propagation distances, be anticipated from your work or that of other investigators?

Whitelaw: I don't think that anyone has answered the very general question in specific terms for the possible range of flows that one can conceive. But I don't think there are any problems with scales of the order of this table or perhaps a bit bigger, for example, in combustion.

D. K. McLaughlin, Oklahoma State University: I have a question about your conclusion that as you increase velocity you need more laser power. I've gone through your ASME paper and you state in there that the number of photons scattered from a particular Doppler wave is inversely proportional to the velocity. The thing is I can't carry that over to the photomultiplier tube because it seems to me that the photomultiplier tube responds to the number photons per unit of time and not per Doppler wave.

Whitelaw: If you take a five milliwatt laser and try to apply it to a supersonic flow, good Luck! It would depend on the instrumentation you use, of course.

P. Iten, Brown Boveri Research Center: I have a small comment on the statement that the photomultiplier will respond to photons per unit time. This is not right, because the photons are used to build up a Doppler cycle. If the cycle is smaller in time for higher flow of course, supersonic flow, then you will not get a good signal because you have less photons per cycle. If you would measure just the

mean value of the scattered light, you were right, but we try to build up a cycle and, therefore, we need a certain voltage per cycle which then defines the signal to noise ratio.

L. L. Lading, Danish Atomic Energy Commission: I might make a comment on this. The photomultiplier is essentially responding to the number of photons per unit time. There's one thing that you have to take into consideration if you want to extract a signal, a Doppler signal has a certain bandwidth. This bandwidth is proportional to the velocity and that means that the (noise) bandwidth of the optimum filter also is proportional to the velocity: i.e. the amount of unwanted noise you take into your signal processing system is proportional to the velocity and therefore the signal to shot noise ratio will decrease in proportion to velocity.

McLaughlin: The second question I had was, have you made any measurements in more highly fluctuating velocity fields? Can the tracker track higher fluctuating velocities?

Whitelaw: In liquids, no. In combustion systems and in air flows, yes, we measured in the recirculation zone, and the burner quart, for example, where you could say the turbulence intensity was 300%. We use Bragg cells to frequency shift. We also measured in the region behind sudden expansion coming through from Reynolds numbers which are very low to Reynolds numbers which are quite sizeable.

G. K. Patterson, University of Missouri-Rolla: What quality steam flows were you studying? Did you mean that they're above 95% quality, 5% moisture by weight? And also what size water droplets were involved here?

Whitelaw: The quality was 95% and above. We didn't try to measure with qualities less than that. The density of the liquid we had in the flow was such that the beam was having trouble getting through. What size were the particles? The easiest answer is that I don't know. I doubt very much that we would have been able to measure had these droplets been significantly greater than 10 microns. You may ask if ten micron particles do follow the flow. I was very careful to say that, I think we were measuring mean velocity and comparing with Pitot tubes and we were not trying at that time to get rms values.

W. W. Fowles, Florida State University: Looking ahead to your comparisons with theoretical and numerical work, I am not at all familiar with what is in the literature in that area, but does it look as if you're within the ball park. Is the factor 2, is it ten per cent, in these comparisons?

Whitelaw: It depends which property you care to talk about. If you talk about mean velocity, you can predict mean velocity in most simple flows by the seat of your pants. It's not very difficult to do. If you talk predictions of normal stresses or shear stress then yes, you're in the right ball park. There are discrepancies and some of the discrepancies have to be resolved.